TSV reveal height and dimension metrology by the TSOM method

Victor Vartanian[a], Ravikiran Attota[b], Haesung Park[b], George Orji[b] and Richard A. Allen[a,b]
[a]SEMATECH, 257 Fuller Road, Suite 2200, Albany, NY, 12203, USA
[b]Semiconductor and Dimensional Metrology Division, National Institute of Standards and Technology, Gaithersburg, MD, 20899, USA

ABSTRACT

This paper reports on an investigation to determine whether through-focus scanning optical microscopy (TSOM) is applicable to micrometer-scale through-silicon via (TSV) reveal metrology. TSOM has shown promise as an alternative inspection and dimensional metrology technique for FinFETs and defects. In this paper TSOM measurements were simulated using 546 nm light and applied to copper TSV reveal pillars with height in the 3 μm to 5 μm range and diameter of 5 μm. Simulation results, combined with white light interferometric profilometry, are used in an attempt to correlate TSOM image features to variations in TSV height, diameter, and sidewall angle (SWA). Simulations illustrate the sensitivity of Differential TSOM Images (DTI's) using the metric of Optical Intensity Range (OIR), for 5 μm diameter and 5 μm height TSV Cu reveal structures, for variation of SWA ($\Delta = 2°$, OIR = 2.35), height (Δ = 20 nm, OIR = 0.28), and diameter (Δ = 40 nm, OIR = 0.57), compared to an OIR noise floor of 0.01.

In addition, white light interferometric profilometry reference data is obtained on multiple TSV reveal structures in adjacent die, and averages calculated for each die's SWA, height, and diameter. TSOM images are obtained on individual TSV's within each set, with DTI's obtained by comparing TSV's from adjacent die. The TSOM DTI's are compared to average profilometry data from identical die to determine whether there are correlations between DTI and profilometry data.

However, with several significant TSV reveal features not accounted for in the simulation model, it is difficult to draw conclusions comparing profilometry measurements to TSOM DTI's when such features generate strong optical interactions. Thus, even for similar DTI images there are no discernible correlations to SWA, diameter, or height evident in the profilometry data. The use of a more controlled set of test structures may be advantageous in correlating TSOM to optical images.

Keywords: TSOM, Through-focus scanning optical microscopy, metrology, TSV, through silicon via, 3D interconnect critical dimension, optical microscopy

1. INTRODUCTION

Through-focus scanning optical microscopy (TSOM) [1-8] allows conventional optical microscopes to collect dimensional information by combining 2D optical images captured at several through-focus positions, transforming a conventional optical microscope into a 3D metrology tool. TSOM is not a resolution enhancement method but an image comparison method and has been demonstrated through simulations to provide lateral and vertical measurement sensitivity of less than a nanometer. This performance is comparable to the dimensional measurement sensitivity of critical dimension (CD) metrology tools such as critical dimension scanning electron microscopy (CD-SEM) and optical critical dimension (OCD). TSOM has shown promise as an inspection and dimensional metrology technique for FinFETs and defects [9], where CD-SEM or bright-field inspection, respectively, are currently used. These simulations indicate that the technique is capable of measuring features far smaller than the diffraction limit of the optical system because TSOM captures much richer data at many z-heights (i.e., through-focus positions) rather than from a single (in-focus) focal plane. Additionally, simulations indicate that TSOM can decouple the measurement of profile dimensional changes at the nanoscale, such as small perturbations in sidewall angle versus height, with little or no ambiguity. For example, simulations have demonstrated sensitivity to nanometer-scale changes in height and diameter. In addition, acquisition time for TSOM is comparable to CD-SEM and OCD.

Metrology, Inspection, and Process Control for Microlithography XXVII, edited by Alexander Starikov, Jason P. Cain,
Proc. of SPIE Vol. 8681, 86812F · © 2013 SPIE · CCC code: 0277-786X/13/$18 · doi: 10.1117/12.2012609

This study investigates the applicability of TSOM to TSV reveal metrology and inspection, and whether TSOM offers advantages relative to other optical techniques that are currently in use for inspection and metrology of TSV reveal structures. This work will present simulations and supporting experiments to demonstrate the application of TSOM to 5 μm diameter TSV Cu reveal features.

2. TSOM IMAGE METHOD

Optics-based metrology tools are advantageous because they have a relatively low cost of ownership, have high throughout, and are usually non-contaminating and non-destructive.

In conventional optical microscopy (such as confocal microscopy), images must usually be acquired at the "best focus" position for a meaningful analysis, since generally the most faithful single image representation of the target is rendered at the best focus position. However, out-of-focus images contain additional useful information about the target. This information can be obtained using an appropriate data acquisition and analysis method. Based on this and on the observation of a distinct signature for different parametric variations, TSOM was introduced, a new method for nanoscale dimensional analysis with sensitivity for 3D nm-sized targets using a conventional brightfield optical microscope. TSOM is applicable to 3D targets (for which a single best focus may be impossible to define), thus enabling it to be used for a wide range of target geometries and application areas.

In the TSOM method, through-focus images are stacked as a function of focus position, resulting in a 3D space containing optical information. From this 3D space, cross-sectional 2D TSOM images are extracted through the location of interest in any given orientation. With TSOM, the entire 3D optical information is acquired and preserved for dimensional analysis. The out-of-focus optical information is not discarded, as in confocal microscopy, nor is the intensity profile reduced to a number, as in the through-focus metric method.

TSOM requires a conventional brightfield optical microscope with a digital camera to capture images and a motorized stage to move the target through the focus. Figure 3 demonstrates the method to construct TSOM images, using an isolated line as an example target. Simulated optical images are used here for illustration. Optical images are acquired as the target is scanned through the focus of the microscope (along the z-axis) as shown in Figures 1(a) and 1(b). Each scan position results in a slightly different 2D intensity image (Figure 1(c)). The optical images are stacked at their corresponding scan positions, creating a 3D TSOM image, for which the x and the y-axes represent the spatial position on the target and the z-axis the scanned focus position. In this 3D space, each location has a value corresponding to its optical intensity. The optical intensities in a plane (e.g., the *xz* plane) passing through the location of interest on the target (e.g., through the center of the line) can be conveniently plotted as a 2D image, resulting in a 2D TSOM image as shown in Figure 1(e), where the x axis represents the spatial position on the target (in x), the y axis represents the focus position, and the color scale represents the optical intensity. Note that the intensity (color) axis is typically rescaled for each image. For 3D targets, appropriate 2D TSOM images are selected for dimensional analysis. In this paper, we use "TSOM image" to refer to these 2D TSOM cross-sectional images.

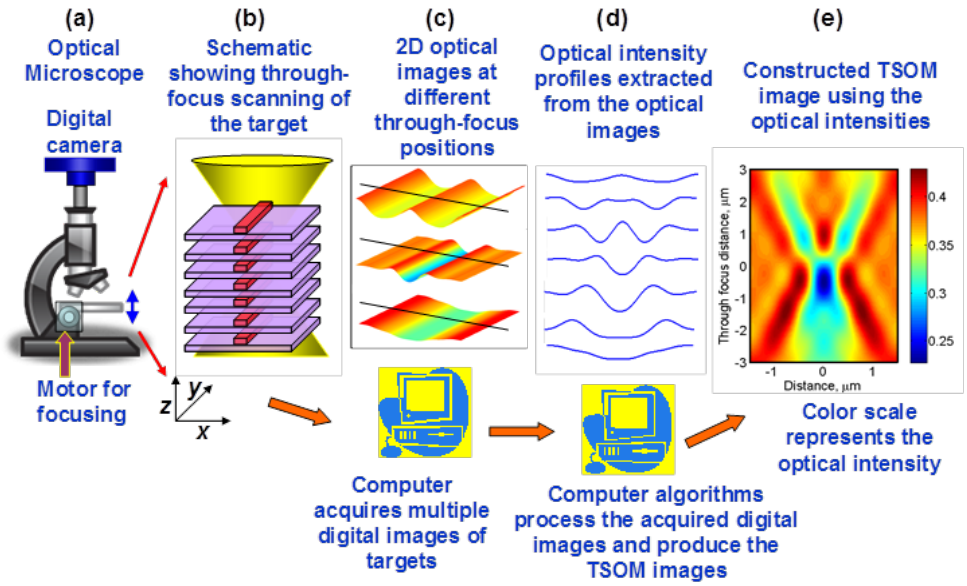

Figure 1. Illustration of method to construct TSOM images using a conventional optical microscope.

As demonstrated in previous work [8], TSOM images are collected as discussed above, and differential TSOM images are calculated to observe the effects of subtle perturbations in the properties of the measurand. Three important properties of TSOM images have been demonstrated:

1. TSOM images change with changes in the target
2. Differential TSOM images appear to be distinct for different types of dimensional changes
3. Differential TSOM images are qualitatively similar for different magnitude differences in the same dimension

Property 1 reflects the sensitivity of the technique to small changes in dimension. Property 2 indicates that the differential TSOM image can act like a "fingerprint" of different types of dimensional perturbations. Property 3 specifies that the magnitude of a given perturbation will scale the magnitude of the differential TSOM image without significantly changing its profile. Such magnitudes can be quantified with an Optical Intensity Range (OIR) metric, which is the absolute range of the differential signal normalized to perfect reflection of the incident illumination.

3. TSOM SELF-CORRELATION COEFFICIENT METHODOLOGY

Application of simulated self-correlation coefficient (SCC) plots at varied azimuth angles is illustrated in Figure 2. Additional information is obtained on anisotropic samples, but is limited to samples that are optically isolated.

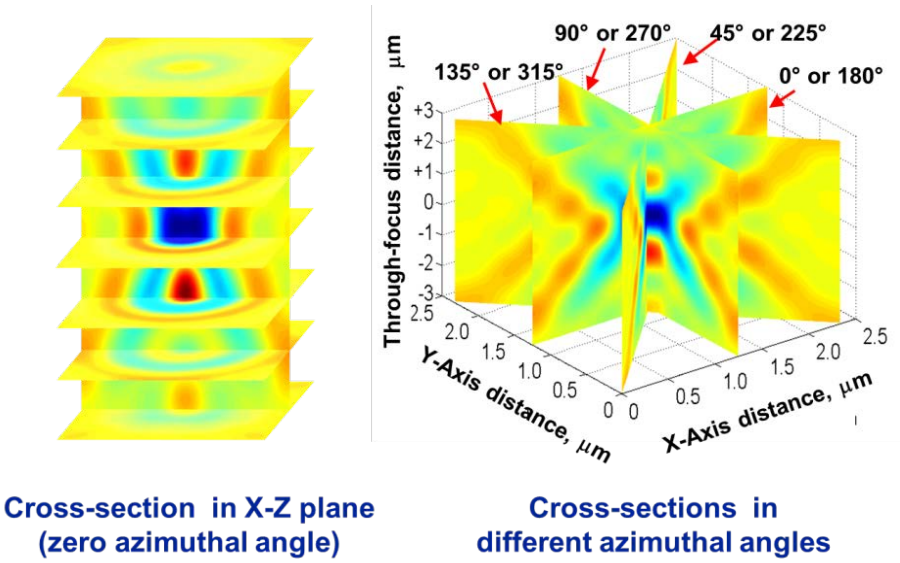

Figure 2. Extraction of TSOM images at different azimuthal angles on a single target.

Figure 3 illustrates simulated SCC plots at varied azimuth angles showing the variable images that can be obtained. The TSOM image obtained at an azimuth angle of 0° is used as the reference image, and additional images obtained at additional azimuthal angles.

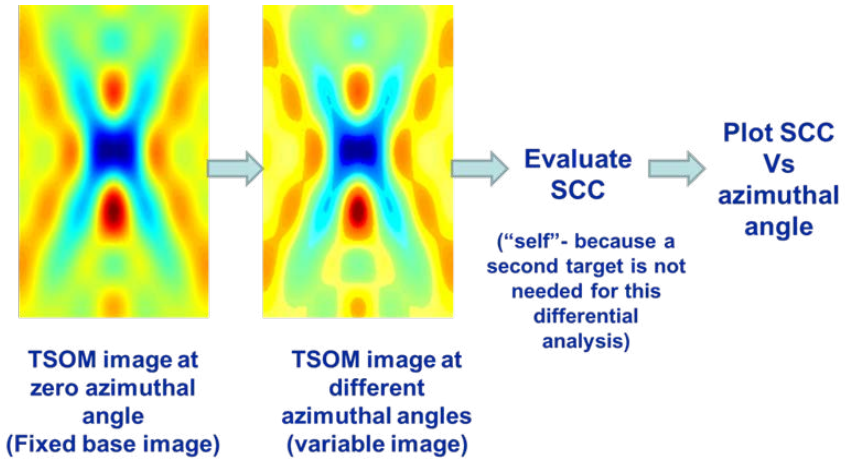

Figure 3. Method to evaluate self-correlation coefficient plots as a function of azimuthal angle.

In Figure 4, simulated SCC plots illustrate sensitivity to TSV Cu reveal shape as shown by the different correlation coefficients as a function of azimuthal angle. The circular shape should nominally yield a straight line. But due to limitations in the simulations conditions (due to pixilation) a slightly distorted SCC profile is shown. However, the elongated Cu reveal exhibits a distinctly different SCC profile, matching the expected behavior.

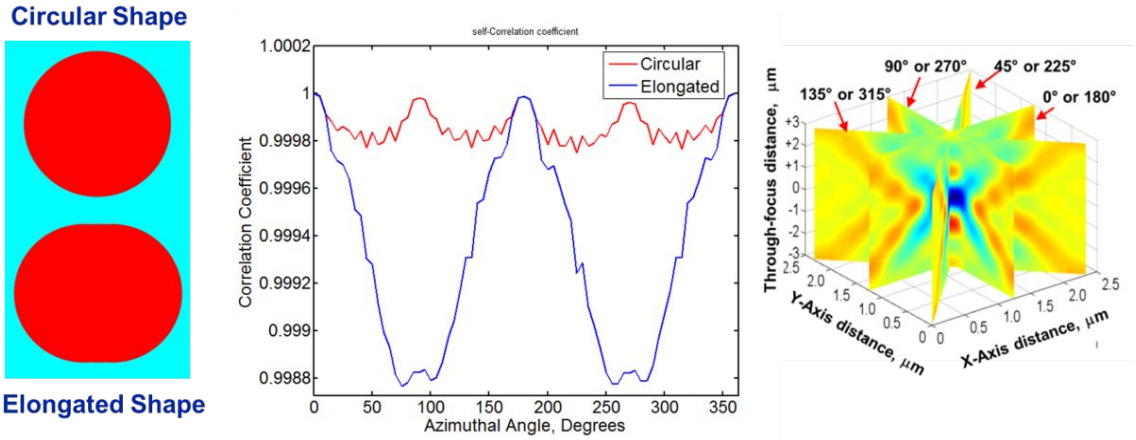

Figure 4. A self-correlation plot indicates sensitivity to TSV shape as shown by the different correlation coefficients as a function of azimuthal angle, showing image variation at various angles. The simulated Cu reveal has 5 µm diameter and height. The non-circular Cu reveal has 200 nm elongation in the x-direction.

4. NOISE THRESHOLD CALCULATION

A simple repeatability experiment was performed to establish the credibility of a 0.1 noise threshold for later comparison to simulated differential TSOM images. Such a comparison can then be used to judge whether a simulated differential image implies that the associated perturbation is distinguishable, thus allowing possible sensitivity limits to be predicted.

Another method of quantifying the noise is to calculate the standard deviation of the intensity values, pixel by pixel. The images shown in Figure 5a and b show the pixel-by-pixel average (0.01) and standard deviation (0.005) for three repeated DTI's of the same measurement using 546 nm illumination. This finding leads to a key assumption for the later simulations: to experimentally detect a dimensional difference, OIR must be > 0.01 of the scaled optical range of the TSOM image.

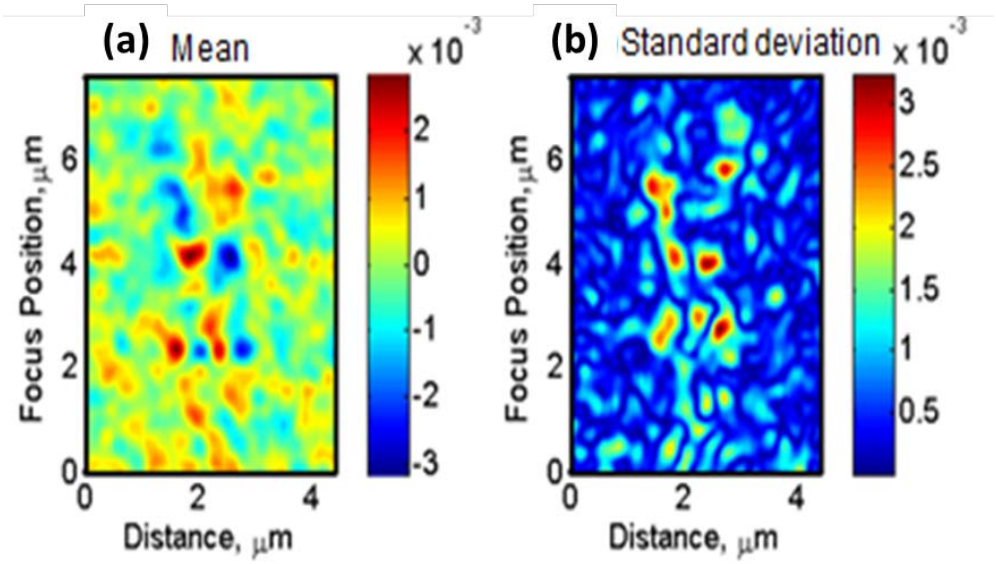

Figure 5. a): Pixel-by-pixel average of three repeat differential TSOM images of the same measurement target. b): Pixel-by-pixel standard deviation of the three repeats. Measurements were obtained with 546 nm illumination. The OIR average is 0.01 and the standard deviation is 0.005.

5. SIMULATIONS & RESULTS ON TSV REVEAL STRUCTURES

To ensure uniform TSV reveal height, methods such as white light interferometry [10-13], laser profiling [14], confocal chromatic imaging [15], and laser triangulation [16] are typically used. Typical optical techniques that are not scatterometry-based do not measure SWA. TSOM has a potential advantage in detecting TSV Cu reveal dimensional changes, especially changes in SWA due to its high sensitivity to SWA change. OIR is an indicator of the magnitude of the difference between two TSOM images, and TSOM's sensitivity to detect that change. The simulations shown in Figure 6 illustrate the sensitivity of the Differential TSOM Images (DTI's) to SWA (D = 2°, OIR = 2.35), height (D = 20 nm, OIR = 0.28), and diameter (D = 40 nm, OIR = 0.57), with a noise floor of 0.01.

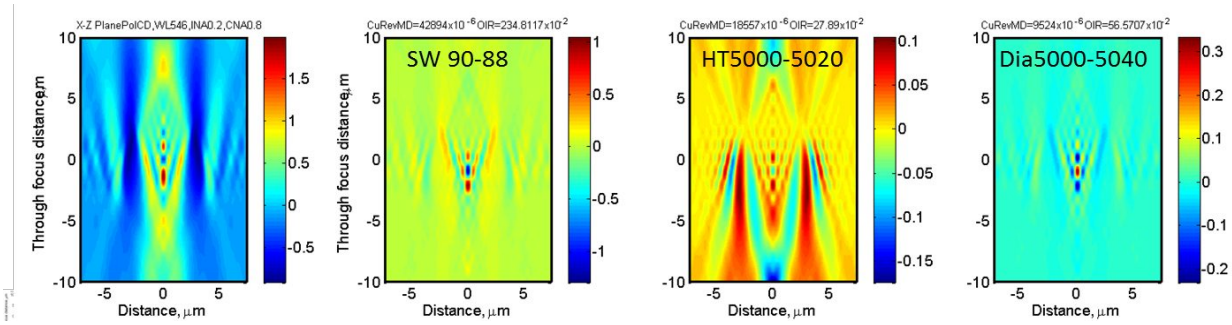

Figure 6. TSOM Image (leftmost) and Differential TSOM Images: Simulations of SWA (Δ = 2°), height (Δ = 20 nm), and diameter (Δ = 40 nm) variation for 5 μm diameter and 5 μm height TSV Cu reveal structures.

6. TSV REVEAL PROCESS

TSV Cu reveal wafers were fabricated using SEMATECH's process flow for 5 μm diameter, 50 μm deep TSVs [17]. Figure 7 a-d shows cross-section diagrams of the back side processing steps. The completed TSV reveal wafers are bonded to a handle wafer to facilitate backside processing (Fig. 7a). Silicon is removed from the back side of the wafer using a grind process, stopping just before reaching the vias (Fig. 7b). A wet etch is used to remove additional silicon (Fig. 7c), leaving the vias protruding from the Si surface. Non-uniformities in the wafer grind process, handle wafer thickness non-uniformity, adhesive layer thickness variation, and the TSV reveal etch process add to cause across-wafer variation in the TSV reveal height. An oxide layer is deposited on the wafer and a chemical-mechanical planarization (CMP) step is used to open the bottom of the vias and planarize the surface (Fig. 7d). This step removes the non-uniformity in the TSV reveal height; however the process window for reveal height variations is limited. Vias not sufficiently revealed will not make electrical contact to the redistribution layer (RDL). Vias with excessive reveal height may be mechanically compromised (or bent) during the CMP. Thus, TSV reveal height and SWA measurement accuracy and precision must be attained by the inspection and metrology system. Tilt SEM images show how the revealed TSVs and the Si surface should appear after etch. They should be clean, free of footings at the base of the TSV, and the silicon surface should not show pyramids or other etching defects (Fig. 8a and b).

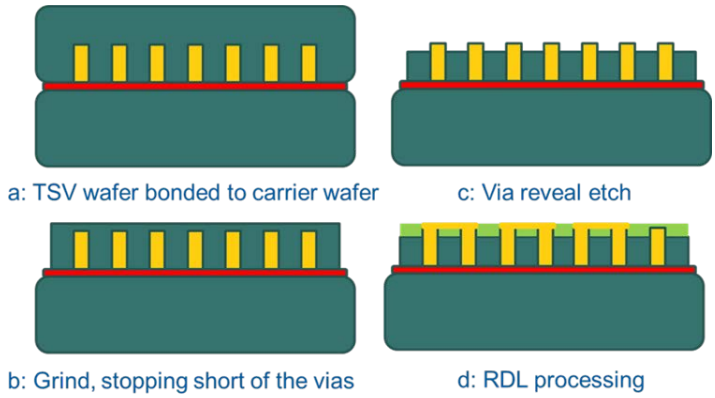

Figure 7 The CMP reveal process includes a) bonding, b) grind, c) wet etch, and d) RDL

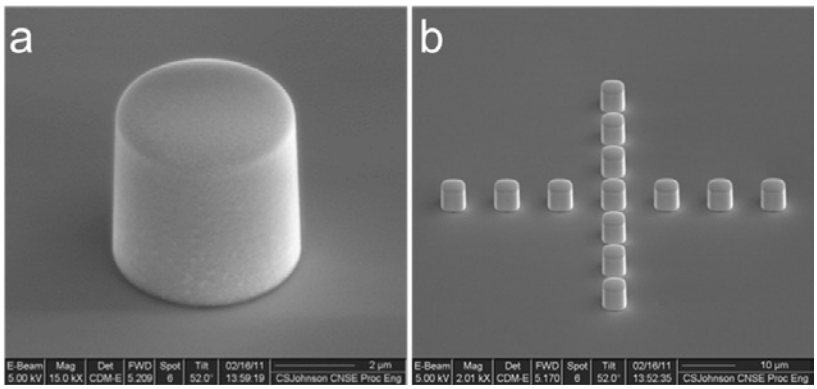

Figure 8. Tilt SEM images showing a 5 µm diameter defect-free Cu TSV reveal structure (a) and array (b) after etch.

7. EXPERIMENTAL TSOM AND PROFILOMETRY MEASUREMENTS

A set of TSV Cu reveal imaging comparisons was made to determine the magnitude of intra-die differences. The DTI's shown in Figure 9 show low OIR's ranging from 0.1 to 0.16, demonstrating that the dimensional differences between TSV Cu reveal structures must be low.

Figure 10 illustrates that TSV intra-die DTI's are qualitatively similar between TSV Cu reveals A-B and A-E, and A-C and A-D, indicating dimensional similarities between TSV reveal structuress in an ensemble of 5 die. Larger dimensional differences can be inferred based on the higher OIR values compared to Fig. 9.

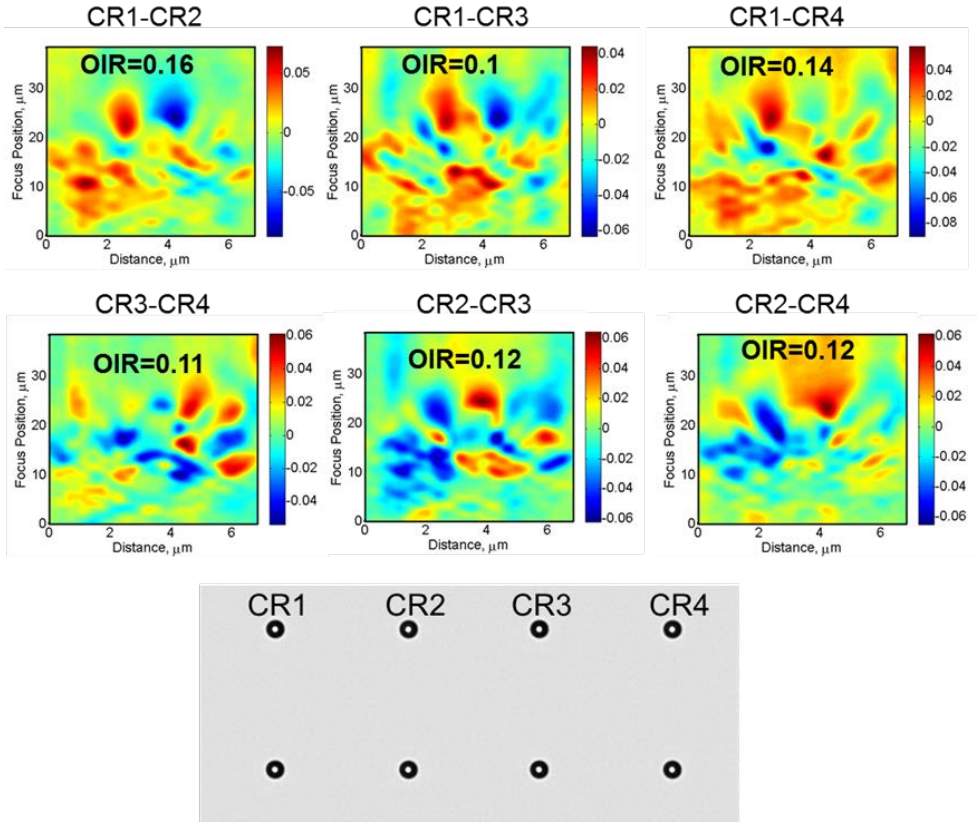

Figure 9. Intra-die dimensional differences appear relatively small, with OIR ranges of 0.1 to 0.16 for TSV reveal structures that are 5 µm diameter and 5 µm height.

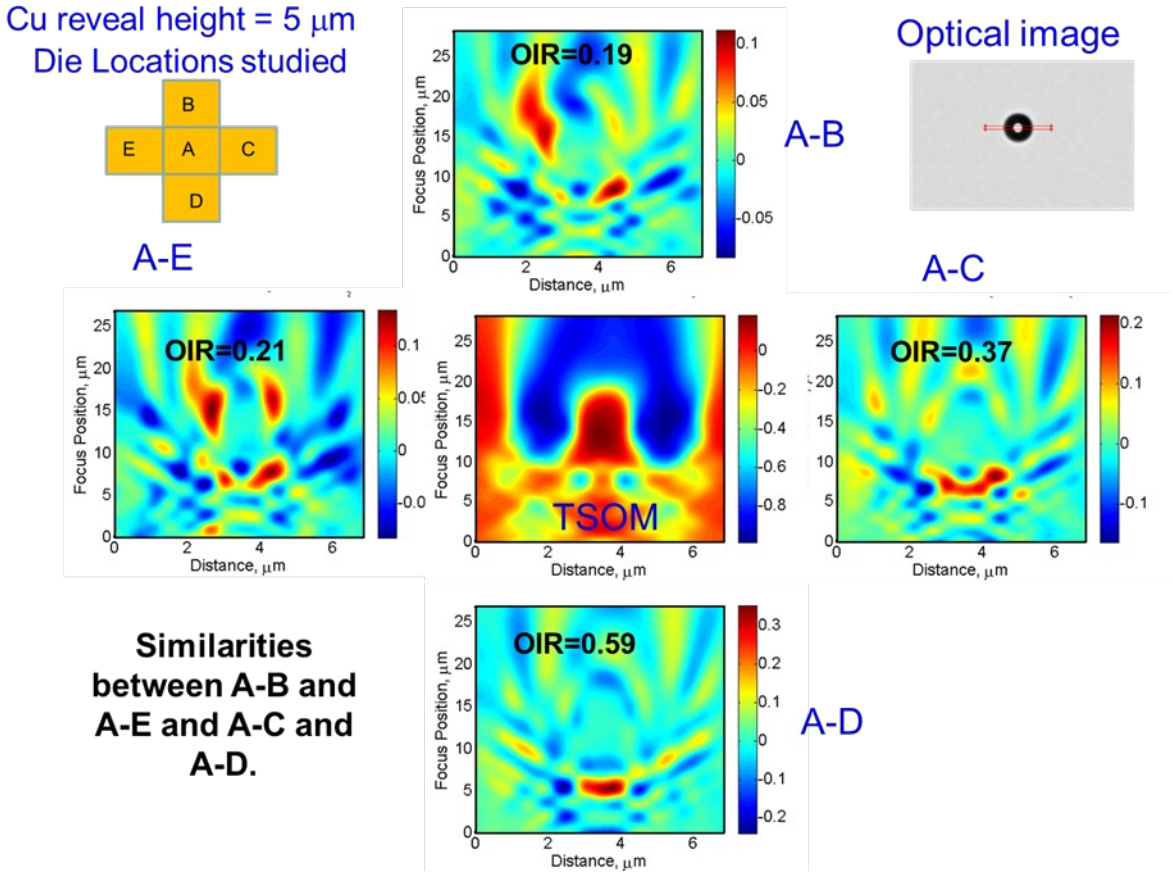

Figure 10. TSV intra-die DTI's are qualitatively similar between TSV reveal A-B and A-E, and A-C and A-D, indicating dimensional similarities between TSV reveal structures in an ensemble of 5 die.

White light interferometric profilometry is a useful technique to obtain TSV reveal dimensions because it is high-speed, accurate, and has an adjustable depth of field. Profilometry measurements were averaged across a 9-TSV reveal unit cell, as shown in Figure 11. TSOM was also used to image individual corresponding TSV reveals from each unit cell in order to correlate the resulting differential TSOM images (DTI) to average unit cell profilometry measurements of TSV reveal height, diameter, and sidewall angle (SWA). The TSV reveal unit cell coordinates used to obtain the individual TSV DTI's and the average unit cell profilometry measurements in the adjacent die locations are shown in Figure 12.

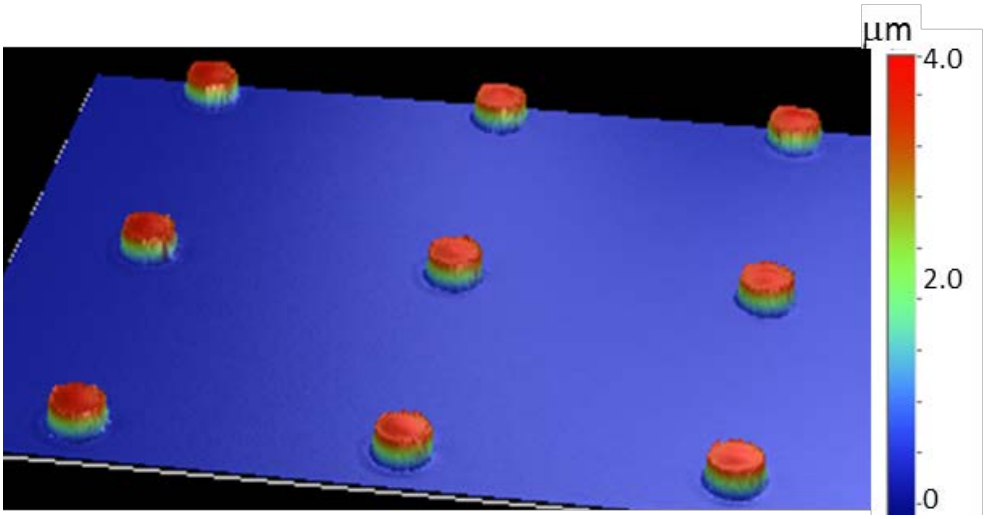

Figure 11. White light interferometric profilometry images illustrating the overall cell layout and reveal heights for a 9-TSV reveal unit cell.

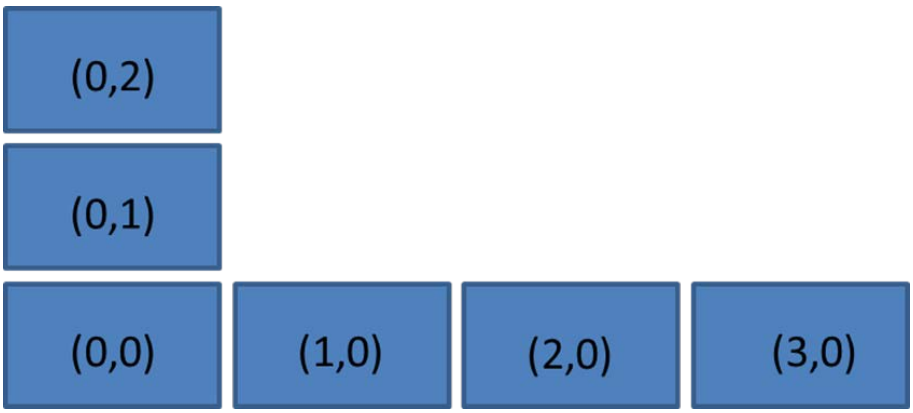

Figure 12. TSV reveal die locations.

8. DISCUSSION

Average profilometry measurements are shown in Table 1 for the 9-TSV reveal unit cell for left and right sidewall angle (LSW and RSW), diameter, and height for reference die location 0,0. Differences between the average profilometry measurements obtained for SWA, diameter, and height for each die location referenced to die 0,0 are shown in Table 2.

TSOM images were also obtained from corresponding individual TSV's in the same 9-TSV reveal unit cells, and their DTI's were obtained by subtraction of one TSV image from another (Figure 12), attempting in software to align the TSOM images in x, y, and z. The OIR's of these DTI's are also included in Table 2 for comparison. Qualitative similarities between DTI's should presumably be correlated to similarities in average profilometry measurements, as the averages of the TSV's are meant to minimize the effects of localized variation between TSV reveal features. Comparison of regions of TSV reveal structures could be one high-speed process control strategy that could identify regions of interest for subsequent in-depth analysis.

8.1. Sensitivity versus specificity

TSOM possesses great sensitivity, but at present, lacks specificity. For example, it is difficult to distinguish between a change in a structural dimension from a change in the surface morphology surrounding the structure or from variation in a film's optical properties. For example, with several significant features not accounted for in Table 1 such as a surface protuberance in the center of the TSV reveal, edge lip, side wall roughness and recess into the Si at the bottom of the TSV reveal (Fig. 13), it is difficult to draw conclusions comparing profilometry measurements to TSOM DTI's. These features could generate strong optical interactions in addition to the parameters listed in the Table 1. Thus, even for similar DTI images such as Figures 14a, b and f, there are no average SWA, diameter, or height similarities that are evident in the profilometry data. The variations between DTI's are likely due to subtle differences in structure, morphology, or material between features.The use of a more controlled set of test structures may be advantageous in correlating TSOM to optical images.

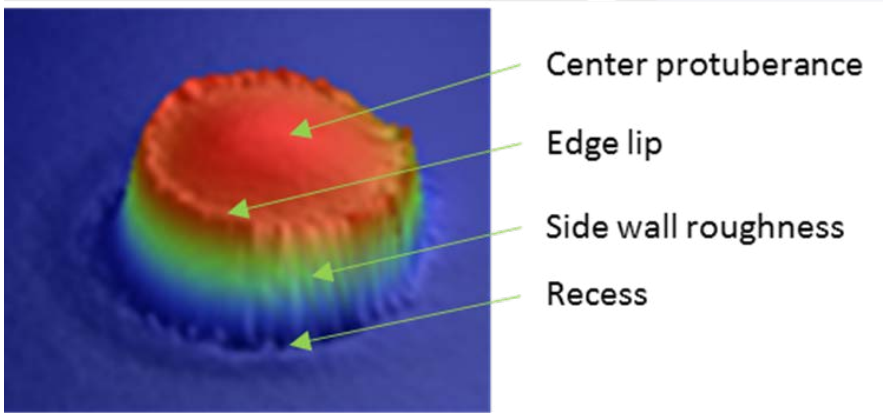

Figure 13. Profilometry image for a TSV reveal feature showing multiple features that were not considered for comparison with TSOM results. These features could result in mismatch between optical profilometry and TSOM measurements.

Table 1. Profilometry measurements (SWA, diameter, and height averages) from unit cell 0,0**.**

Die	LSW (°)	RSW (°)	Dia. (nm)	Height (nm)
0,0	84.44	86.27	3758	3708
	84.9	85.73	3645	3704
	85.57	85.07	3753	3678
	85.14	86.44	3738	3703
Average	**84.97**	**85.69**	**3718**	**3698**
Average SWA	**85.33**			

Table 2. Differences in the average unit cell dimensions of Cu TSV's measured using white light interferometric profilometry and individual DTI OIR results**.**

DTI Image	Die Coordinate	White Light Interferometry			TSOM
		SWA (°)	Diameter (nm)	Height (nm)	Avg. OIR
a	(0,0)-(0,1)	4.0	-80.5	-127.4	26.3
b	(0,0)-(0,2)	0.6	28.6	-767.4	31.7
c	(0,1)-(0,2)	-3.4	109.1	-640.1	12.0
d	(0,0)-(1,0)	1.2	-32.4	-477.3	12.8
e	(0,0)-(2,0)	3.1	-124.3	-345.9	15.7
f	(0,0)-(3,0)	1.8	-125.3	-546.7	28.5

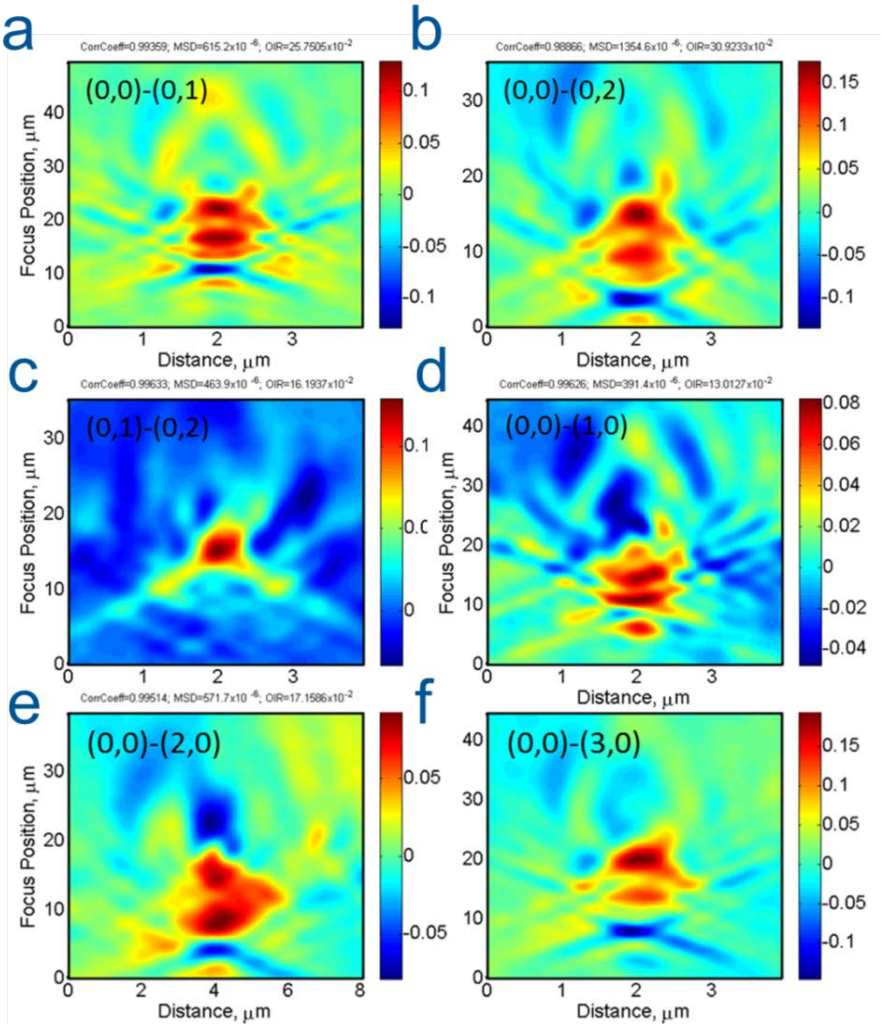

Figure 14. DTI's obtained from TSV reveal images and their associated die coordinate origins. The variations between DTI's are likely due to subtle differences in structure, morphology, or material between features.

9. SUMMARY

Simulations indicate that TSOM is sensitive to nanometer-scale changes in SWA, CD, and height on 5 μm diameter and 5 μm height TSV Cu reveal structures. The data reported in this study demonstrated this sensitivity; however, the presence of subtle features significantly influenced the TSOM results on real structures, masking the general dimensional variations observed by white light interferometric profilometry. In the future, simulations would need to be modified to include additional dimensional parameters such as top profile, edge lip, sidewall roughness, and bottom sidewall recess (and possibly others), as well as additional material parameters such as liner, barrier, and seed layer, including their associated optical properties. This further work is necessary to better understand how well TSOM images can be correlated to dimensional changes of real TSVs, and to assess how useful TSOM will be to complement other metrology techniques.

ACKNOWLEDGEMENTS

The authors would like to thank John Kramar and Andras Vladar, NIST, and Larry Smith and Klaus Hummler, SEMATECH, for valuable discussions, and Robert Edgeworth, Iqbal Ali, Craig Huffman, Steve Olson, Pete Moschak, Harry Lazier, and Elizabeth Lorenzini, SEMATECH, for wafer fabrication.

REFERENCES

[1] Attota, R., Silver R.M., and Potzick, J., "Optical illumination and critical dimension analysis using the through-focus focus metric," Proc. SPIE, Vol. 6289, 62890Q (2006).
[2] Attota, R., Silver, R.M., and Barnes, B.M., "Optical through-focus technique that differentiates small changes in line width, line height, and sidewall angle for CD, overlay, and defect metrology applications," Proc. SPIE, Vol. 6922, 6922OE (2008).
[3] Brown, E., "Nanoscale dimensioning is fast, cheap with new NIST optical technique," NIST Tech Beat (2008). http://www.nist.gov/public_affairs/techbeat/tb2008_1028.htm#tsom
[4] Attota, R., Germer, T.A., and Silver, R.M., "Through-focus scanning-optical-microscope imaging method for nanoscale dimensional analysis," Optics Letters, Vol. 33, Issue 17, 1990-1992 (2008).
[5] Attota, R., Germer, T.A., and Silver, R.M., "Nanoscale measurements with a t hrough-focus scanning optical microscope," Future Fab, 30, 83-88 (2009).
[6] Attota, R., and Silver, R.M., "Nanometrology using a through-focus scanning optical microscopy method," Meas. Sci. Technol. 22, 024002 (2011).
[7] Attota, R., "Nanoscale Measurements with the TSOM Optical Method," an on-line presentation from NIST, (2011). http://www.nist.gov/pml/div683/grp03/upload/tsom-ravikiran-attota.pdf.
[8] Attota, R., Dixson, R.G., Kramar, J.A., Potzick, J.E., Vladar, A.E., Bunday, B., Rudack, A., and Novak, E., "TSOM method for semiconductor metrology," Proc. SPIE, Vol. 7971, 79710T (2011).
[9] Arceo, A., Bunday, B., Vartanian, V., and Attota, R. "Patterned Defect & CD Metrology by TSOM Beyond the 22 nm Node," Proc. SPIE, Vol. 8324, 832401 (2012).
[10] Wyant, J., "Computerized Interferometric Measurement of Surface Microstructure," Proc. SPIE, Vol. 2576, 122-130 (1995).
[11] P. Hariharan, [Optical Interferometry], 2nd ed.," Elsevier Science, 151-157 (2003).
[12] J. Wyant, 'White Light Interferometry," Proc. SPIE, Vol. 4737, 98-107 (2002).
[13] P. de Groot and L. Deck, "Three-dimensional Imaging by Sub-Nyquist Sampling of White-light Interferograms," Opt. Lett., vol. 18, no. 17, 1462–1464 (1993).
[14] Lindow, J., Bennett, S., Smith, I., "Scanned Laser Imaging For Integrated Circuit Metrology," Proc. SPIE, Vol. 0565, 81-87 (1986)
[15] Tiziani, H., and Uhde, H.-M., "Three-Dimensional Image Sensing by Chromatic Confocal Microscopy," Appl. Optics, Vol. 33, Issue 10, 1838-1843 (1994).
[16] Asgari, R., "3-D Laser Metrology: Supporting Micro-Bump Technology," Advanced Packaging, Aug./Sep., 2008.
[17] Olson, S.; Hummler, K., "TSV reveal etch for 3D integration," 2011 IEEE International 3D Systems Integration Conference (3DIC), 1-4, Jan. 31 2012-Feb. 2 2012.